INTERNATIONAL JOURNAL FOR NUMERICAL METHODS IN FLUIDS
Int. J. Numer. Meth. Fluids 2007; **55**:713–721
Published online 20 March 2007 in Wiley InterScience (www.interscience.wiley.com). DOI: 10.1002/fld.1471

Dynamics of Jovian atmospheres with applications of nonlinear singular vector method

Zhiyue Zhang[1,*,†] and Jing Lin[2]

[1] *School of Mathematics and Computer Science, Nanjing Normal University, Nanjing 210097, China*
[2] *Department of Marine, Earth, and Atmospheric Sciences, North Carolina State University, Raleigh, NC 27695, U.S.A.*

SUMMARY

Nonlinear singular vectors (NSVs) of a Jovian atmosphere model are obtained numerically in this paper. NSVs are the initial perturbation, whose nonlinear evolution attains the maximal value of the cost function, which is constructed according to the physical problem of interest. The results demonstrate that the motions of Jupiter's atmosphere is relatively stable under some assumptions. Copyright © 2007 John Wiley & Sons, Ltd.

Received 31 March 2005; Revised 1 February 2007; Accepted 1 February 2007

KEY WORDS: nonlinear singular vector; finite difference; optimization; Jupiter; Earth

1. INTRODUCTION

In the solar system, motions in the planetary atmospheres are mainly divided into two kinds of problems: the terrestrial problem and the Jovian problem. Earth's atmospheric motion and Jupiter's atmospheric motion are the typical representatives of these problems. Major factors that contribute to the complexity of Earth's weather are its irregular mountain ranges and the fact that the atmospheric eddies and the planet are comparable in size. In contrast, Jupiter's atmosphere comes pre-idealized, since there are no mountain ranges, air–sea interfaces, and surface drag, or surface temperature gradients [1]. Ever since Galileo discovered spots on the sun by telescope

*Correspondence to: Dr Zhiyue Zhang, School of Mathematics and Computer Science, Nanjing Normal University, Nanjing 210097, China.
†E-mail: zhangzhiyue@njnu.edu.cn

Contract/grant sponsor: National Natural Science Foundation of China; contract/grant number: 10471067
Contract/grant sponsor: Natural Science Foundation of Jiangsu Provincial Education Department; contract/grant number: 2005101TSJB156
Contract/grant sponsor: Jiangsu Provincial Government Scholarship for Overseas Studies and Jiangsu Provincial NSF; contract/grant number: BK2006215

in 1609, the study of motion in planetary atmospheres has attracted significant attention. There are no continents or oceans to interfere with the flow of gas in Jupiter's atmosphere. Jupiter's atmospheric motions, which depend on different scales, display different forms, such as turbulence on the smaller scale and steady zonal currents on the larger scale, while the Great Red Spot on intermediate scales. Because of their vastly different scales, the various phenomena probably lie in different dynamic regimes [2]. There has been many significant previous research about the motion in planetary atmospheres, including Jupiter ([3–5] and their references) and many models have been proposed to explain the motion of Jupiter and Earth ([6–8] and their references). Further understanding of planetary motions and improvement in predictability of planetary atmospheres are of continuing interest [9, 10]. A more detailed statement of the current understanding in this area can be found in Majda and Wang [3].

Predictability and sensitivity of atmospheric motions are the central problems in both theoretical and numerical research of atmospheric science. One approach to attack these problems is to investigate the evolution of initial perturbations, which usually represent the initial uncertainties. The fast growing initial perturbations have the largest impact on the uncertainties of prediction, and often play a dominant role in the variation of motions. Determination of the fastest growing initial perturbations has been an important issue since the work of Lorenz [11]. After Lorenz, a series of works, such as Farrell [12], Buizza and Palmer [13], Tziperman and Ioannou [14] and Frederiksen [15, 16], allowed mathematical and atmospheric researchers to recognize the value and applicability of linear singular vector (LSV) in meteorology and physical oceanography. The linear approach assumes that the initial perturbation is sufficiently small such that its evolution can be governed approximately by the tangent linear model of the nonlinear model and the computation of the (linear) fastest growing perturbation is reduced to the calculation of LSV. However, it is well known that the motion of the atmosphere or the ocean is governed by complicated nonlinear systems. In order to reveal the essential nonlinear character of the motion of the atmosphere and ocean, a new concept of nonlinear singular vector (NSV) was proposed by Mu [17], which is a natural generalization to the classical LSV.

In this paper, the NSVs of a nonlinear, quasigeostrophic, barotropic, model of Jupiter's and Earth's atmosphere is obtained by solving a numerical nonlinear optimization problem, which provides a step towards the application of NSV to the more general and realistic model in studying Jupiter's and Earth's atmospheric motions. The main goal of this paper is that we treat only the simplest dynamical problems, using them as a test of the new and complicated method. On Jupiter, the typical wind speed U is $100\,\mathrm{m\,s^{-1}}$ and typical length scale L is about $10\,000\,\mathrm{km}$, we may consider it is reasonable for larger scale. The gravitational acceleration g is $26\,\mathrm{m\,s^{-2}}$. On Earth, both U and L are $10\,\mathrm{m\,s^{-1}}$ and $1000\,\mathrm{km}$, respectively, and g is about $9.8\,\mathrm{m\,s^{-2}}$. In a later paper, we will apply the framework to a three-dimensional nonlinear primitive equation model.

This paper is organized as follows. In Section 2, the model and the concept of NSV are described. In Section 3, a numerical experiment is presented.

2. THE MODEL AND THE NSV

We consider the following non-dimensional, two-dimensional, quasigeostrophic model:

$$\frac{\partial P}{\partial t} + \partial(\Phi, P) = f$$

DOI: 10.1002/fld

$$P = \nabla^2\Phi - F\Phi + f_0 + \frac{f_0}{H}h_s \quad \text{in } \Omega\times[0, T]$$

$$\Phi|_{t=0} = \Phi_0 \tag{1}$$

where P is the potential vorticity, Φ is the stream function, f is the external forcing, f_0 is the Coriolis parameter, H is the characteristic depth and h_s is the topography. F is the planetary Froude number:

$$F = \left(\frac{L}{L_R}\right)^2 = \frac{f_0^2 L^2}{gH(1-\rho_1/\rho_2)}$$

where L_R is the Rossby deformation radius, L is the length scale, and ρ_1 and ρ_2 are the density of the upper and lower atmosphere, respectively ($\rho_1<\rho_2$). The Jacobian operator $\partial(\Phi, P) = \Phi_x P_y - \Phi_y P_x$. $\Omega = [0, X]\times[0, Y]$ with double periodic boundary conditions, which may be considered to be reasonable for large scale. The beta effect is also neglected because we consider the simplest theoretical model which is mathematically tractable. For fixed $T>0$ and initial condition $\Phi|_{t=0} = \Phi_0$, the propagator M is well defined, i.e. $\Phi(x, y, T) = M(\Phi_0)$ is the solution of (1) at time T [18].

Let Φ_T and $\Phi_T + \varphi_N$ be the solutions of (1) with initial value Φ_0 and $\Phi_0+\varphi_0$, i.e.

$$\Phi_T = M(\Phi_0), \quad \Phi_T + \varphi_N = M(\Phi_0+\varphi_0) \tag{2}$$

Energy norm is widely employed [19–21] in the study of predictability, which is defined as

$$\|\Phi\|^2 = \int_\Omega (|\nabla\Phi|^2 + F|\Phi|^2)\,dx\,dy \tag{3}$$

where Φ is the stream function.

The nonlinear optimal perturbation φ_0^* is the maximum of the functional $J(\varphi_0)$, i.e.

$$J(\varphi_0^*) = \max J(\varphi_0) \tag{4}$$

where

$$J(\varphi_0) = \frac{\|M(\Phi_0+\varphi_0) - M(\Phi_0)\|}{\|\varphi_0\|} = \frac{\|\varphi_N\|}{\|\varphi_0\|} \tag{5}$$

and φ_N presents the nonlinear evolution of the initial perturbation φ_0.

To calculate the nonlinear optimal perturbation, we consider

$$J_1(\varphi_0) = [J(\varphi_0)]^2 = \frac{\|M(\Phi_0+\varphi_0) - M(\Phi_0)\|^2}{\|\varphi_0\|^2} \tag{6}$$

Obviously,

$$J_1(\varphi_0^*) = \max J_1(\varphi_0) \tag{7}$$

To capture the maximum of $J_1(\varphi_0)$, we calculate the minimum of

$$J_2(\varphi_0) = \frac{1}{J_1(\varphi_0)} = \frac{\|\varphi_0\|^2}{\|M(\Phi_0+\varphi_0) - M(\Phi_0)\|^2} \tag{8}$$

DOI: 10.1002/fld

The first variation of $J_2(\varphi_0)$ is

$$\delta J_2(\varphi_0) = \frac{2((-\nabla^2 + F)\varphi_0, \delta\varphi_0)\|M(\Phi_0+\varphi_0) - M(\Phi_0)\|^2}{\|M(\Phi_0+\varphi_0) - M(\Phi_0)\|^4} - \frac{((-\nabla^2 + F)(M(\Phi_0+\varphi_0) - M(\Phi_0)), \mathbf{M}(\Phi_0+\varphi_0)\delta\varphi_0)\|\varphi_0\|^2}{\|M(\Phi_0+\varphi_0) - M(\Phi_0)\|^4} \tag{9}$$

where $\mathbf{M}(\Phi_0+\varphi_0)$ is the tangent linear approximation of propagator M at $\Phi_0+\varphi_0$.

Let $\mathbf{M}^*$ be the adjoint operator of $\mathbf{M}$, we have

$$\delta J_2(\varphi_0) = \frac{2((-\nabla^2 + F)\varphi_0, \delta\varphi_0)\|M(\Phi_0+\varphi_0) - M(\Phi_0)\|^2}{\|M(\Phi_0+\varphi_0) - M(\Phi_0)\|^4} - \frac{(\mathbf{M}^*(\Phi_0+\varphi_0)(-\nabla^2 + F)(M(\Phi_0+\varphi_0) - M(\Phi_0)), \delta\varphi_0)\|\varphi_0\|^2}{\|M(\Phi_0+\varphi_0) - M(\Phi_0)\|^4} \tag{10}$$

Determination of the NSVs of models for the atmospheric dynamics, usually result in nonlinear optimization problems of high dimension. It is too difficult to obtain analytical solutions, hence we adopt a numerical approach. To obtain the nonlinear optimal perturbation numerically, the discretization of the operator M is carried out. In our numerical approach, the Arakawa finite difference scheme [22] is used to discretize the Jacobian operator. The temporal discretization is carried out by using a second-order Adams–Bashforth scheme, which damp the computational mod [23], and the stream function Φ is treated as an unknown term, and the potential vorticity P is calculated by using the second equation of (1). The familiar five-point difference scheme is employed to discretize the Laplacian operator.

The limited memory BFGS method, which is an extension of the conjugate gradient method, is used to solve our optimization problem. This method is suitable for large-scale optimization problems because the amount of storage required by the algorithm and thus the cost of the iteration can be controlled by the user. In the research of data assimilation and numerical weather forecast and physical oceanography, this method has been successfully applied for solving the related optimization problems with higher dimensions. The detailed description of this algorithm can be found in Dong and Nocedal [24].

3. NUMERICAL RESULTS

Jupiter is the largest planet in the solar system, much larger than Earth, and is mostly made of hydrogen. Its radius is 71 492 km, rotation period is about 9.92 Earth hours. For mathematical simplicity, we take $f=0$ and neglect the beta effect. Our numerical results are not sensitive to changes several times in Froude number. We choose randomly the initial perturbations and make the size of perturbation within several times of energy norm of basic state in the computational process. If the size is too large, this will lose physical meanings. In this section, we take the Jupiter space domain $\Omega=[0, 6.4]\times[0, 3.2]$, which corresponds to the dimensional case $[0, 64\,000\,\text{km}]\times[0, 32\,000\,\text{km}]$. The model parameters in non-dimensional form are chosen as follows: $F=0.2584$, $f_0=10$. Because there are liquid state and no mountain ranges on the surface of Jupiter, the topographs

DOI: 10.1002/fld

Table I. The nonlinear evolutions of NSV and NSV for 1, 3, 7, and 10 Jupiter days, respectively.

	1 Jupiter days	3 Jupiter days	7 Jupiter days		10 Jupiter days	
$\|\varphi_0^*\|$	2.2705E − 2	8.6043E − 3	1.7316E − 3	2.3765	8.5080E − 4	2.7061
$\|\varphi_N\|$	6.2088E − 2	5.1723E − 2	2.1808E − 2	6.3976	2.3942E − 2	6.8546

$h_s = 0$ for the Jovian case. The space step $d = 0.2$ corresponding to a dimensional length of 2000 km and the time step $dt = 0.006$ corresponding to $t = 10$ Earth minutes.

The experiment is for the basic flow $\Phi_0 = 1.0 \times (\sin(2\pi y/3.2) + 0.25)$. The energy norm of the basic flow is $\|\Phi_0\| = 6.4769$. $T = 59$, 177, 413 and 590 (corresponding to 1, 3, 7, and 10 Jupiter days) are the time steps of Jupiter, respectively. We use the NSV method to calculate the nonlinear fastest growing perturbation, the detail results are demonstrated in the Table I.

The numerical results of 1, 3, 7 and 10 Jupiter days are summarized in Table I. $\|\Phi_0\|$, $\|\varphi_0^*\|$, and $\|\varphi_N\|$, are presented in Table I, where $\|\varphi_0^*\|$ and $\|\varphi_N\|$ are the energy norm of NSV and the norms of nonlinear evolution of NSV, respectively. $\|\varphi_N\|$ is obtained by integrating the nonlinear model with NSV as initial values. The initial perturbations are chosen randomly, but their energy norms are not greater than several times of that of the basic state. In fact, if the initial perturbations are too large, they will lose physical meaning. We find one global maxima of functional $J(\varphi_0)$ for 1 and 3 Jupiter days and one global and one local maxima of functional $J(\varphi_0)$ for 7 and 10 Jupiter days, respectively. It follows from Table I that the nonlinear evolutions of global nonlinear optimal perturbations (GNOPs) φ_0^* are 6.2088E − 2, 5.1723E − 2, 2.1808E − 2 and 2.3942E − 2 for 1, 3, 7, 10 Jupiter days, respectively. With the time increasing from 1 to 10 Jupiter days, the nonlinear evolution of NSV φ_0^* are on the same order of magnitude. On the other hand, the nonlinear evolution of the local nonlinear optimal perturbations (LNOPs) φ_0^* for 7 and 10 Jupiter days are 6.3976 and 6.8546, respectively. We find that LNOP plays a more important role than the GNOP; this result is the same as the results in Mu and Wang [25]. From 7 to 10 Jupiter days, the nonlinear evolution of LNOPs are 6.3976 and 6.8546, and there is not a remarkable difference between LNOP for 7 and 10 Jupiter days. These results imply that the motion of Jupiter's atmosphere is relatively stable under the given assumptions. In the following contour figures, we used three types of contour lines: solid, dotted and dashed to distinguish positive, zero, and negative contour values.

Figure 1(a) and (b) are NSVs for 1 and 3 Jupiter days, respectively. Figure 1 shows the case of short time. Figure 2(a) and (b) are NSVs for 7 and 10 Jupiter days, respectively. The case of long time is shown in Figure 2. It is clear from Figure 1 that there are no remarkable differences between the case of 1 and 3 Jupiter days. The characteristics of NSV for the case of 7 and 10 Jupiter days are similar with that of the case of 1 and 3 Jupiter days. Both Figures 1 and 2 show that almost the same initial perturbation reach the maximum evolution after 1 and 3 Jupiter days, and 7 and 10 Jupiter days, respectively. This indicates that the Jovian atmosphere is relatively stable. It is worthwhile to point out that in the nonlinear case, there exists a local maximum due to the nonlinearity. Now that LNOPs play a more important role in the study of predictability. We show that evolutions of LNOP for 7 Jupiter days and LNOP for 10 Jupiter days in Figure 3. We also find that there is not a significant difference between LNOPs for 7 Jupiter days and 10 Jupiter days. Furthermore, this implies that the Jovian atmosphere is relatively stable.

In order to compare the difference between two atmospheric motion, we also give the numerical results for the Earth. The experiment for the Earth is for the basic flow $\Phi_0 = 1.0 \times (\sin(2\pi y/3.2) +$

DOI: 10.1002/fld

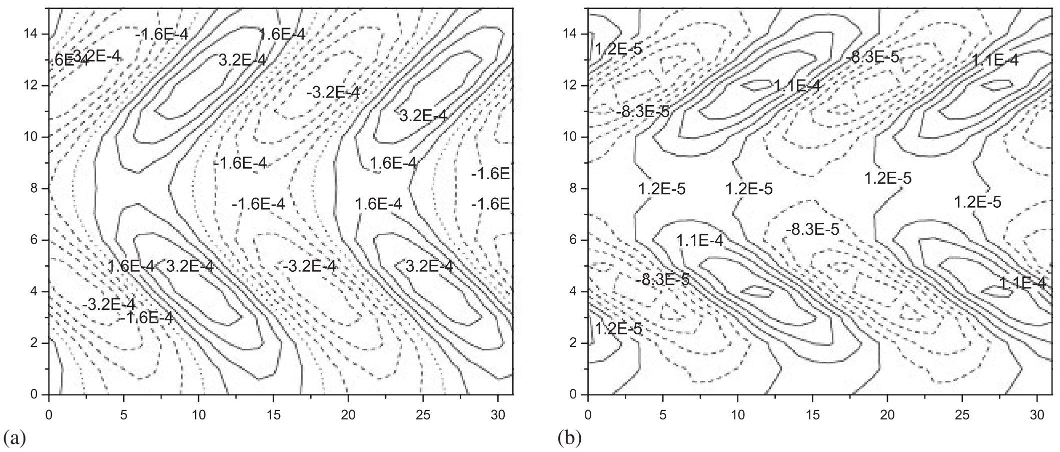

Figure 1. Results of nonlinear singular vector for different Jupiter days: (a) NSV with energy norm 2.2705E − 2 for 1 Jupiter day and (b) NSV with 8.6043E − 3 for 3 Jupiter days. The interval values of contour in (a) and (b) are 8.0E − 5 and 4.75E − 5, respectively.

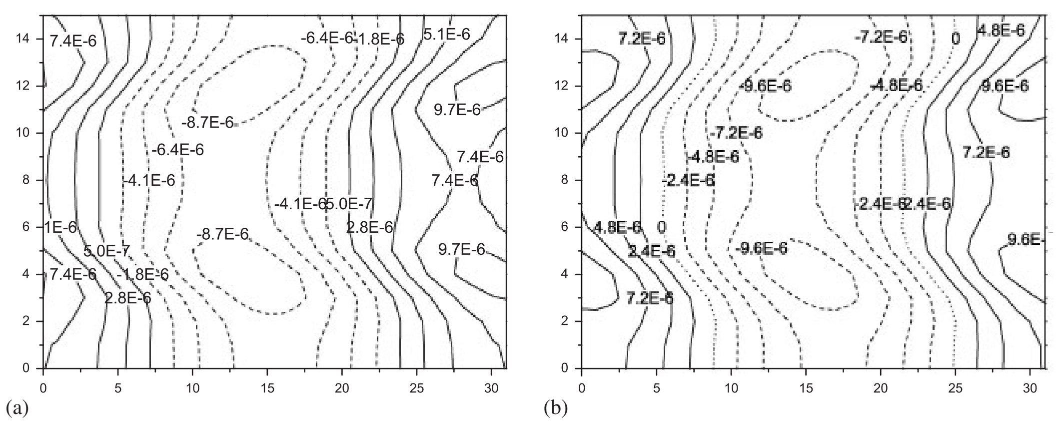

Figure 2. Results of nonlinear singular vector for different Jupiter days: (a) NSV with energy norm 1.7316E − 3 for 7 Jupiter days and (b) NSV with 8.5080E − 4 for 10 Jupiter days. The interval values of contour in (a) and (b) are 2.0E − 5 and 2.4E − 6, respectively.

0.25) which is the same as the case of Jupiter. The Earth topography $h_s = 1.0 \times \sin(2\pi y/3.2)$, $1/H = 0.35$. The parameter $F = 0.1$, the other parameters for Earth and Jupiter are the same as given above. The energy norm of the basic flow is $\|\Phi_0\| = 6.4769$.

$T = 720$ (corresponding to 5 Earth days) are the time steps of Earth and Jupiter. We use the nonlinear optimal perturbation method to calculate the NSV, the detailed results are demonstrated in the Table II.

In Table II, there are local nonlinear optimal perturbations in the case of Earth or Jupiter because of nonlinearity. The growth rates λ_E for Earth vary considerably from 9.1173 to 5.4667, but the

DOI: 10.1002/fld

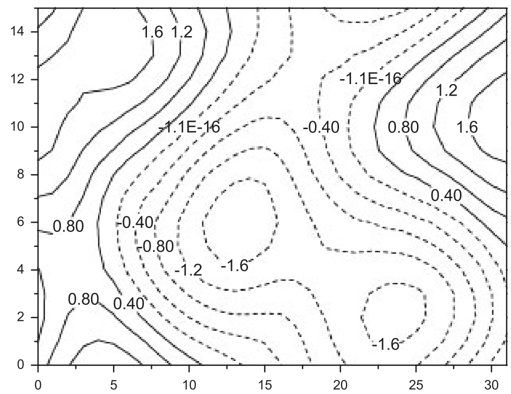

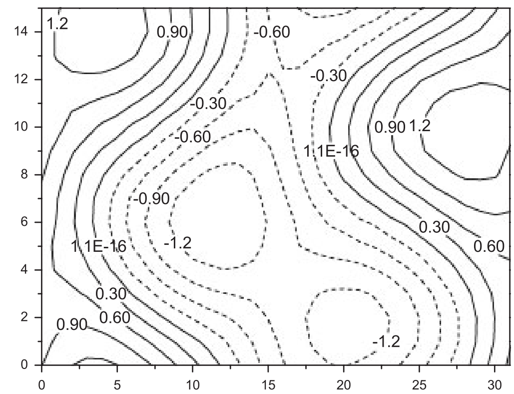

Figure 3. Results of LNOP for different Jupiter days: (a) evolution of LNOP with energy norm 2.3765 for 7 Jupiter days and (b) evolution of LNOP with 2.7061 for 10 Jupiter days. The interval values of contour in (a) and (b) are 0.3 and 0.4, respectively.

Table II. The comparison of growth rates between Jupiter and Earth for 5 Earth days.

	$i=1$	$i=2$	$i=3$	$i=4$
Earth				
λ_E^i	9.1173	7.4032	5.4667	—
$\|\varphi_0^*\|$	2.986E − 4	9.651E − 1	1.5643	—
Jupiter				
$\|\varphi_0^*\|$	1.56E − 4	8.976E − 1	1.4269	2.5063
λ_J^i	6.2049	6.1097	6.1340	5.9889

growth rates λ_J for Jupiter are almost constant and only change from 6.2049 to 5.9889. This implies that Earth's atmosphere motion is more unstable than Jupiter's.

Local nonlinear optimal perturbations for the Earth and Jupiter are presented in Figure 4. Figure 4(a) and (b) are the LNOPs with $\|\varphi_0\| = 9.651\text{E}-1$ and 1.5643 in the case of Earth, respectively. There are remarkable differences between Figure 4(a) and (b). The LNOPs with $\|\varphi_0\| = 8.976\text{E}-1$ and 1.4269 in the case of Jupiter are shown in Figure 4(c) and (d), respectively, but they are very similar.

It is well known that Earth's atmosphere receives more energy per unit area than any other planetary atmosphere, and yet has the weakest winds in the solar system [1]. Mu and Zhang [26] demonstrate that we should consider the nonlinear effects in the study of atmospheric and oceanic motions. Although the statement is based on the somewhat artificial assumption of the model, this may not present the realistic status of Jupiter's atmosphere. However, the test results coincide with some of the ones in Williams [27] and Conrath *et al.* [5]. In particular, the application of the NSV method to the theoretical model of motion in Jupiter's and Earth's atmosphere may provide an opportunity to better understand the motions of Jupiter's and Earth's atmosphere. A nonlinear optimal perturbation method was used to investigate the Jovian atmosphere, and make a comparison

DOI: 10.1002/fld

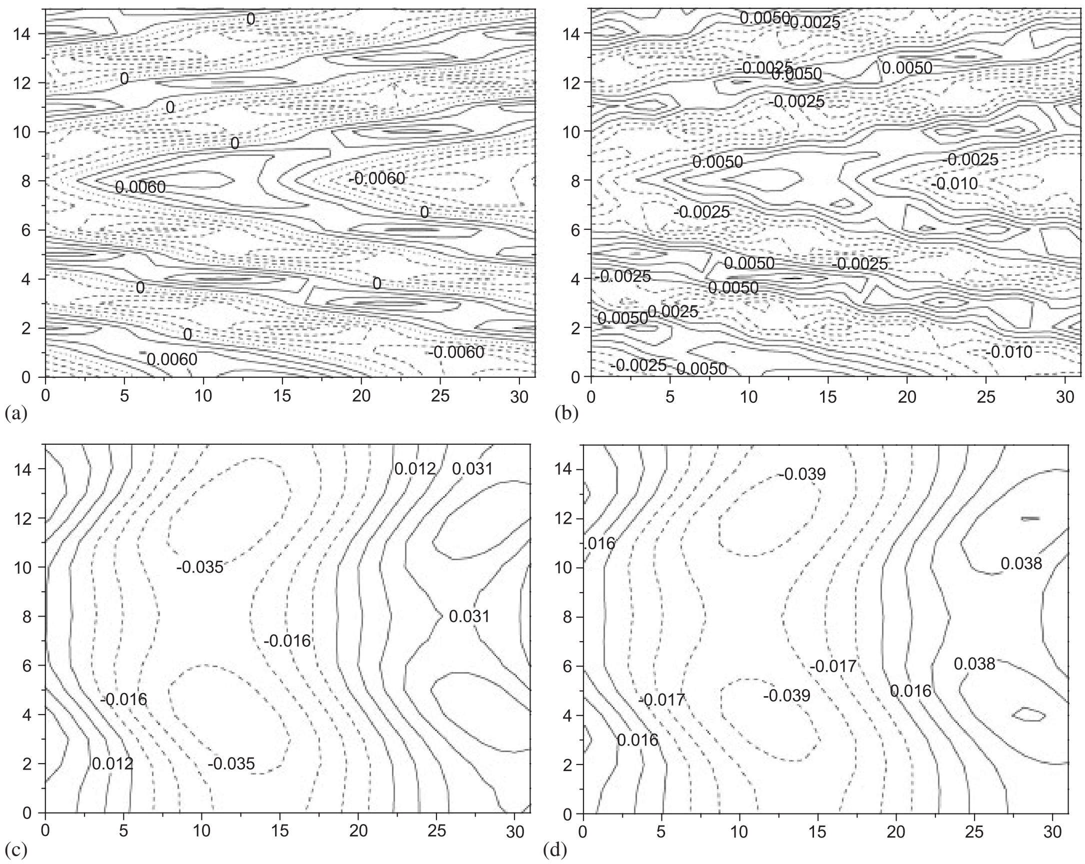

Figure 4. Results of LNOP for Earth and Jupiter: (a) LNOP for Earth with energy norm 9.651E − 1 for 5 Earth days; (b) LNOP for Earth with 1.5643 for 5 Earth days; (c) LNOP for Jupiter with energy norm 8.976E − 1 for 5 Earth days; (d) LNOP for Jupiter with 1.4269 for 5 Earth days. The interval values of contour in the figures (a)–(d) are 0.002, 0.00375, 0.0095 and 0.011, respectively.

with Earth's atmosphere. This is an indication that the terrestrial problem is complicated. Major factors that contribute to the complexity of Earth's weather are its irregular boundary conditions, i.e. its mountain ranges. This motivates the further investigation of the complex dynamics of Jupiter's and Earth's atmospheres.

ACKNOWLEDGEMENTS

The authors would like to thank two anonymous reviewers for their many suggestions to improve this paper. The first author would like to thank Prof. Mu Mu and Prof. Zhilin Li for their many help. He would also like to thank Prof. Charlie M. Elliott and Prof. Kewei Zhang for their kindness in providing good work facilities when he visited the U.K.

REFERENCES

1. Dowling TE. Dynamics of Jovian atmospheres. *Annual Review of Fluid Mechanics* 1995; **27**:293–334.
2. Williams GP, Yamagata T. Geostrophic regimes, intermediate solitary vortices and Jovian eddies. *Journal of the Atmospheric Sciences* 1984; **41**:453–478.
3. Majda A, Wang XM. *Nonlinear Dynamics and Statistical Theories for Basic Geophysical Flows*. Cambridge University Press: Cambridge, 2006.
4. Williams GP. Planetary circulations: 1. Barotropic representation of Jovian and terrestrial turbulence. *Journal of the Atmospheric Sciences* 1978; **35**:1399–1426.
5. Conrath BJ, Gierasch PJ, Nath N. Stability of zonal flows on Jupiter. *Icarus* 1981; **48**:256–282.
6. Ingersoll AP, Guong PG. Numerical model of long-lived Jovian vortices. *Journal of the Atmospheric Sciences* 1981; **38**:2067–2076.
7. Achterberg RK, Ingersoll AP. A normal-mode approach to Jovian atmospheric dynamics. *Journal of the Atmospheric Sciences* 1989; **46**:2448–2462.
8. Taylor FW. The Jovian system from the Galileo Jupiter orbiter. *Journal of the British Interplanetery Society* 2001; **54**:147–152.
9. Ingersoll AP, Pollard D. Mothin in the interiors and atmospheres of Jupiter and Saturn: scale analysis, anelastic equations, barotropic stability criterion. *Icarus* 1982; **52**:62–80.
10. Simmons AJ, Hollingsworth A. Some aspects of the improvement in skill of numerical weather prediction. *Quarterly Journal of the Royal Meteorological Society* 2002; **128**:647–677.
11. Lorenz EN. A study of the predictability of a 28-variable atmosphere model. *Tellus* 1965; **17**:321–333.
12. Farrell BF. Optimal excitation of baroclinic waves. *Journal of the Atmospheric Sciences* 1989; **46**:1193–1206.
13. Buizza R, Palmer T. The singular vector structure of the atmospheric global circulation. *Journal of Atmospheric Sciences* 1995; **52**:1434–1456.
14. Tziperman E, Ioannou PJ. Transient growth and optimal excitation of thermohaline variability. *Journal of Physical Oceanography* 2002; **32**:3427–3435.
15. Frederiksen JS. Adjoint sensitivity and finite-time normal mode disturbances during block. *Journal of the Atmospheric Sciences* 1997; **54**:1144–1165.
16. Frederiksen JS. Singular vectors, finite-time normal modes and error growth during blocking. *Journal of the Atmospheric Sciences* 2000; **57**:312–333.
17. Mu M. Nonlinear singular vectors and nonlinear singular values. *Science in China*(*D*) 2000; **43**:375–385.
18. Mu M, Zeng QC. New development on existence and uniqueness of solutions to some models in atmospheric dynamics. *Advances in Atmospheric Sciences* 1991; **8**:383–398.
19. Xue Y, Cane MA, Zebiak SE. Predictability of a coupled model of ENSO using singular vector analysis. Part I: optimal growth in seasonal background and ENSO cycles. *Monthly Weather Review* 1997; **125**:2043–2056.
20. Xue Y, Cane MA, Zebiak SE, Palmer TN. Predictability of a coupled model of ENSO using singular vector analysis. Part II: optimal growth and forecast skill. *Monthly Weather Review* 1997; **125**:2057–2073.
21. Ehrendorfer M. The total energy norm in a quasigeostrophic model. *Journal of the Atmospheric Sciences* 2000; **57**:3443–3451.
22. Liao DX, Wang LM. *Principle of Numerical Weather Forecasting and its Applications* (*in Chinese*). Meteorology Press: Beijing, 1986; 146–148.
23. Haltiner GJ, Williams RT. *Numerical Prediction and Dynamic Meteorology* (2nd edn). Wiley: Chichester, U.K., 1980; 477.
24. Dong CL, Nocedal J. On the limited BFGS method for large scale optimization. *Mathematical Programming* 1989; **45**:503–566.
25. Mu M, Wang JC. Nonlinear fastest growing perturbation and the first kind of predictability. *Science in China*(*D*) 2001; **44**:1128–1139.
26. Mu M, Zhang ZY. Conditional nonlinear optimal perturbations of a two-dimensional quasigeostrophic model. *Journal of the Atmospheric Sciences* 2006; **63**:1587–1604.
27. Williams GP. Jovian dynamics. Part I: vortex stability, structure, and genesis. *Journal of Atmospheric Sciences* 1996; **53**:2685–2734.

DOI: 10.1002/fld